

CEO stabilized frequency comb from a 1- μm Kerr-lens mode-locked bulk Yb:CYA laser

Zijiao Yu,¹ Hainian Han,¹ Yang Xie,² Yingnan Peng,² Xiaodong Xu,³ and Zhiyi Wei^{1,*}

¹ Beijing National Laboratory for Condensed Matter Physics, Institute of Physics, Chinese Academy of Sciences, Beijing 100190, China

² School of Physics and Optoelectronics Engineering, Xidian University, Xi'an 710071, China

³ Jiangsu Key Laboratory of Advanced Laser Materials and Devices, School of Physics and Electronic Engineering, Jiangsu Normal University, Xuzhou 221116, China

*zywei@iphy.ac.cn

Abstract: We report the first Kerr-lens mode-locked (KLM) bulk frequency comb in the 1- μm spectral regime. The fundamental KLM Yb:CYA laser is pumped by a low-noise, high-bright 976-nm fiber laser and typically provides 250-mW output power and 57-fs pulse duration. Only 58-mW output pulses were launched into a 1.3-m photonic crystal fiber (PCF) for one octave-spanning supercontinuum generation. Using a simplified collinear f - $2f$ interferometer, the free-running carrier-envelope offset (CEO) frequency was measured to be 42-dB signal-to-noise ratio (SNR) for a 100-kHz resolution and 9.6-kHz full width at half maximum (FWHM) under a 100-Hz resolution. A long-term CEO control at 23 MHz was ultimately realized by feeding the phase error signal to the pump power of the oscillator. The integrated phase noise (IPN) of the locked CEO was measured to be 316 mrad with an integrated range from 1 Hz to 10 MHz. The standard deviation and Allan deviation for more than 4-hour recording are 1.6 mHz and 5.6×10^{-18} (for 1-s gate time), respectively. This is, to the best of our knowledge, the best stability achieved among the 1- μm solid-state frequency combs.

©2016 Optical Society of America

OCIS codes: (320.0320) Ultrafast optics; (140.3615) Lasers, ytterbium; (140.0140) Lasers and laser optics; (320.6629) Supercontinuum generation; (320.7150) Ultrafast spectroscopy.

References and links

1. S. A. Diddams, "The evolving optical frequency comb," *J. Opt. Soc. Am. B* **27**(11), B51–B62 (2010).
2. S. T. Cundiff and J. Ye, "Femtosecond optical frequency combs," *Rev. Mod. Phys.* **75**(1), 325–342 (2003).
3. A. Schliesser, N. Picque, and T. W. Hansch, "Mid-infrared frequency combs," *Nat. Photonics* **6**(7), 440–449 (2012).
4. D. J. Jones, S. A. Diddams, J. K. Ranka, A. Stentz, R. S. Windeler, J. L. Hall, and S. T. Cundiff, "Carrier-envelope phase control of femtosecond mode-locked lasers and direct optical frequency synthesis," *Science* **288**(5466), 635–639 (2000).
5. A. Cingöz, D. C. Yost, T. K. Allison, A. Ruehl, M. E. Fermann, I. Hartl, and J. Ye, "Direct frequency comb spectroscopy in the extreme ultraviolet," *Nature* **482**(7383), 68–71 (2012).
6. C. Benko, T. K. Allison, A. Cingöz, L. Hua, F. Labaye, D. C. Yost, and J. Ye, "Extreme ultraviolet radiation with coherence time greater than 1 s," *Nat. Photonics* **8**(7), 530–536 (2014).
7. T. Udem, R. Holzwarth, and T. W. Hänsch, "Optical frequency metrology," *Nature* **416**(6877), 233–237 (2002).
8. C. H. Li, A. J. Benedick, P. Fendel, A. G. Glenday, F. X. Kärtner, D. F. Phillips, D. Sasselov, A. Szentgyorgyi, and R. L. Walsworth, "A laser frequency comb that enables radial velocity measurements with a precision of 1 cm s^{-1} ," *Nature* **452**(7187), 610–612 (2008).
9. M. Hentschel, R. Kienberger, C. Spielmann, G. A. Reider, N. Milosevic, T. Brabec, P. Corkum, U. Heinzmann, M. Drescher, and F. Krausz, "Attosecond metrology," *Nature* **414**(6863), 509–513 (2001).
10. F. L. Hong, K. Minoshima, A. Onae, H. Inaba, H. Takada, A. Hirai, H. Matsumoto, T. Sugiura, and M. Yoshida, "Broad-spectrum frequency comb generation and carrier-envelope offset frequency measurement by second-harmonic generation of a mode-locked fiber laser," *Opt. Lett.* **28**(17), 1516–1518 (2003).
11. T. R. Schibli, I. Hartl, D. C. Yost, M. J. Martin, A. Marcinkevicius, M. E. Fermann, and J. Ye, "Optical frequency comb with submillihertz linewidth and more than 10 W average power," *Nature* **2**(6), 355–359 (2008).
12. A. Ruehl, A. Marcinkevicius, M. E. Fermann, and I. Hartl, "80 W, 120 fs Yb-fiber frequency comb," *Opt. Lett.* **35**(18), 3015–3017 (2010).

13. L. S. Ma, Z. Bi, A. Bartels, L. Robertsson, M. Zucco, R. S. Windeler, G. Wilpers, C. Oates, L. Hollberg, and S. A. Diddams, "Optical frequency synthesis and comparison with uncertainty at the 10^{-19} level," *Science* **303**(5665), 1843–1845 (2004).
14. T. M. Fortier, A. Bartels, and S. A. Diddams, "Octave-spanning Ti:sapphire laser with a repetition rate >1 ghz for optical frequency measurements and comparisons," *Opt. Lett.* **31**(7), 1011–1013 (2006).
15. R. Holzwarth, M. Zimmermann, T. Udem, T. W. Hänsch, P. Russbüldt, K. Gäbel, R. Poprawe, J. C. Knight, W. J. Wadsworth, and P. St. J. Russell, "White-light frequency comb generation with a diode-pumped Cr:LiSAF laser," *Opt. Lett.* **26**(17), 1376–1378 (2001).
16. K. Kim, B. R. Washburn, G. Wilpers, C. W. Oates, L. Hollberg, N. R. Newbury, S. A. Diddams, J. W. Nicholson, and M. F. Yan, "Stabilized frequency comb with a self-referenced femtosecond Cr:forsterite laser," *Opt. Lett.* **30**(8), 932–934 (2005).
17. S. A. Meyer, J. A. Squier, and S. A. Diddams, "Diode-pumped Yb:KYW femtosecond laser frequency comb with stabilized carrier-envelope offset frequency," *Eur. Phys. J. D* **48**(1), 19–26 (2008).
18. M. C. Stumpf, S. Pekarek, A. E. H. Oehler, T. Südmeyer, J. M. Dudley, and U. Keller, "Self-referencable frequency comb from a 170-fs, 1.5- μ m solid-state laser oscillator," *Appl. Phys. B* **99**(3), 401–408 (2010).
19. S. Schilt, N. Bucalovic, V. Dolgovskiy, C. Schori, M. C. Stumpf, G. D. Domenico, S. Pekarek, A. E. H. Oehler, T. Südmeyer, U. Keller, and P. Thomann, "Fully stabilized optical frequency comb with sub-radian CEO phase noise from a SESAM-modelocked 1.5- μ m solid-state laser," *Opt. Express* **19**(24), 24171–24181 (2011).
20. S. Pekarek, T. Südmeyer, S. Lecomte, S. Kundermann, J. M. Dudley, and U. Keller, "Self-referencable frequency comb from a gigahertz diode-pumped solid-state laser," *Opt. Express* **19**(17), 16491–16497 (2011).
21. A. Klenner, M. Golling, and U. Keller, "A gigahertz multimode-diode-pumped Yb:KGW enables a strong frequency comb offset beat signal," *Opt. Express* **21**(8), 10351–10357 (2013).
22. C. J. Saraceno, S. Pekarek, O. H. Heckl, C. R. E. Baer, C. Schriber, M. Golling, K. Beil, C. Kränkel, G. Huber, U. Keller, and T. Südmeyer, "Self-referenceable frequency comb from an ultrafast thin disk laser," *Opt. Express* **20**(9), 9650–9656 (2012).
23. A. Klenner, F. Emaury, C. Schriber, A. Diebold, C. J. Saraceno, S. Schilt, U. Keller, and T. Südmeyer, "Phase-stabilization of the carrier-envelope-offset frequency of a SESAM modelocked thin disk laser," *Opt. Express* **21**(21), 24770–24780 (2013).
24. C. A. Zaugg, A. Klenner, M. Mangold, A. S. Mayer, S. M. Link, F. Emaury, M. Golling, E. Gini, C. J. Saraceno, B. W. Tilma, and U. Keller, "Gigahertz self-referenceable frequency comb from a semiconductor disk laser," *Opt. Express* **22**(13), 16445–16455 (2014).
25. O. Pronin, M. Seidel, F. Lücking, J. Brons, E. Fedulova, M. Trubetskov, V. Pervak, A. Apolonski, T. Udem, and F. Krausz, "High-power multi-megahertz source of waveform-stabilized few-cycle light," *Nat. Commun.* **6**, 6988 (2015).
26. H. A. Haus and A. Mecozi, "Noise of mode-locked lasers," *IEEE J. Quantum Electron.* **29**(3), 983–996 (1993).
27. K. L. Corwin, N. R. Newbury, J. M. Dudley, S. Coen, S. A. Diddams, K. Weber, and R. S. Windeler, "Fundamental noise limitations to supercontinuum generation in microstructure fiber," *Phys. Rev. Lett.* **90**(11), 113904 (2003).
28. W. Zhang, H. Han, Y. Zhao, Q. Du, and Z. Wei, "A 350 MHz Ti:sapphire laser comb based on monolithic scheme and absolute frequency measurement of 729 nm laser," *Opt. Express* **17**(8), 6059–6067 (2009).
29. W. D. Tan, D. Y. Tang, X. D. Xu, D. Z. Li, J. Zhang, C. W. Xu, and J. Xu, "Femtosecond and continuous-wave laser performance of a diode-pumped Yb³⁺:CaYAlO₄ laser," *Opt. Lett.* **36**(2), 259–261 (2011).
30. W. Tian, Z. Wang, L. Wei, Y. Peng, J. Zhang, Z. Zhu, J. Zhu, H. Han, Y. Jia, L. Zheng, J. Xu, and Z. Wei, "Diode-pumped Kerr-lens mode-locked Yb:LYSO laser with 61 fs pulse duration," *Opt. Express* **22**(16), 19040–19046 (2014).
31. Z. Yu, H. Han, J. Zhang, L. Hou, Y. Xie, and Z. Wei, "Kerr-lens mode-locked Yb³⁺:CaYAlO₄ laser and octave-spanning supercontinuum generation," in *Advanced Solid State Laser Conference*, OSA Technical Digest (online) (Optical Society of America, 2015), paper AM5A.25.
32. A. Vernaleken, B. Schmidt, M. Wolferstetter, T. W. Hänsch, R. Holzwarth, and P. Hommelhoff, "Carrier-envelope frequency stabilization of a Ti:sapphire oscillator using different pump lasers," *Opt. Express* **20**(16), 18387–18396 (2012).
33. R. P. Scott, T. D. Mulder, K. A. Baker, and B. H. Kolner, "Amplitude and phase noise sensitivity of modelocked Ti:sapphire lasers in terms of a complex noise transfer function," *Opt. Express* **15**(14), 9090–9095 (2007).
34. T. D. Mulder, R. P. Scott, and B. H. Kolner, "Amplitude and envelope phase noise of a modelocked laser predicted from its noise transfer function and the pump noise power spectrum," *Opt. Express* **16**(18), 14186–14191 (2008).
35. M. Hoffmann, S. Schilt, and T. Südmeyer, "CEO stabilization of a femtosecond laser using a SESAM as fast opto-optical modulator," *Opt. Express* **21**(24), 30054–30064 (2013).
36. B. H. Kolner, "Dynamic temperature distribution in cylindrical laser rods with time-varying pump sources," *IEEE J. Sel. Top. Quant. Electron.* **18**(1), 486–493 (2012).
37. R. Paschotta, A. Schlatter, S. C. Zeller, H. R. Telle, and U. Keller, "Optical phase noise and carrier-envelope offset noise of mode-locked lasers," *Appl. Phys. B* **82**(2), 265–273 (2006).
38. Y. Jiang, Z. Bi, L. Robertsson, and L. S. Ma, "A collinear self-referencing set-up for control of the carrier-envelope offset frequency in Ti:sapphire femtosecond laser frequency combs," *Metrologia* **42**(4), 304–307 (2005).
39. Z. Yu, H. Han, L. Hou, and Z. Wei, "Carrier-envelope phase stabilized octave-spanning laser with monolithic scheme," in *2015 Conference on Lasers and Electro-optics Pacific Rim* (Optical Society of America, 2015), paper 26F3_3.

40. W. Zhang, M. Lours, M. Fischer, R. Holzwarth, G. Santarelli, and Y. Coq, "Characterizing a fiber-based frequency comb with electro-optic modulator," *IEEE Trans. Ultrason. Ferroelectr. Freq. Control* **59**(3), 432–438 (2012).
 41. C. C. Lee, C. Mohr, J. Bethge, S. Suzuki, M. E. Fermann, I. Hartl, and T. R. Schibli, "Frequency comb stabilization with bandwidth beyond the limit of gain lifetime by an intracavity graphene electro-optic modulator," *Opt. Lett.* **37**(15), 3084–3086 (2012).
 42. S. Koke, C. Grebing, H. Frei, A. Anderson, A. Assion, and G. Steinmeyer, "Direct frequency comb synthesis with arbitrary offset and shot-noise-limited phase noise," *Nat. Photonics* **4**(7), 462–465 (2010).
-

1. Introduction

Self-referenced optical frequency combs (OFC) from femtosecond mode-locked lasers have revolutionized the fields of precision measurements in frequency and time [1–3] since their birth at the end of 1990s [4]. Nowadays, high-precision OFCs are widely used in numerous frontier research areas and greatly promote the development of relevant scientific branches. In molecular metrology field, the spectra of OFCs have extended to the extreme ultraviolet regime [5,6] and mid-infrared regime through different techniques [3,7]. In astronomical spectroscopy, the introduction of OFCs with high repetition rates considerably improved the precision of the radial velocity measurement [8]. In attosecond science, OFCs enable precision control over the electric field of the ultrashort laser, which makes it possible to generate attosecond pulses and achieve attosecond time-resolved measurement of the molecular dynamics process [9].

These increasing application requirements, on the other hand, stimulate the appearance of novel frequency combs based on different kinds of laser sources. Among them, fiber based OFCs have been applied widely due to their long-term operation and compact structures [10]. As technology improved, fiber OFCs with high output power and short pulse duration were also demonstrated [11,12]. However, high material dispersion, high nonlinear effect and low Q-factor laser cavity in the fiber OFCs will introduce a large amount of optical phase noise, especially for the fiber systems with high power scaling. By contrast, self-referenced solid-state frequency combs have considerable attractions due to their low intrinsic noise, flexible structures and high averaging power of the oscillators [13,14]. Here in Fig. 1, we classify the existing solid-state frequency combs in terms of emission wavelength and pulse duration of the fundamental laser sources [15–25]. We notice that all the KLM bulk frequency combs (red square) throughout the entire wavelength regime have the shortest pulse duration, which indicates wider output spectra and more available longitudinal modes for subsequent application. Relevant researches reveal that KLM oscillators have intrinsically better potential for a very low CEO noise compared to other kinds of mode-locked mechanism [26]. In addition, supercontinuum generated from nonlinear fiber has also been verified to have a better coherence for oscillators with shorter pulse duration [27].

Despite of various advantages, only several kinds of KLM bulk frequency combs were realized so far owing to the lack of suitable laser source. In the visible to 800-nm regime, Ti:sapphire laser based frequency comb is no doubt the most widely employed. Excellent properties and mature techniques make it even a standard instrument and commercially available in many applications [28]. In 900-nm and 1.3- μm , KLM Cr-doped bulk lasers — Cr:LiSAF and Cr:forsterite — were reported to be harnessed as the comb fundamental lasers [15,16]. For the 1- μm regime, however, though dozens of Yb-doped laser bulk oscillators were realized over the last decade years [29,30], most of them were limited by either low output power or long pulse duration to be developed towards frequency combs.

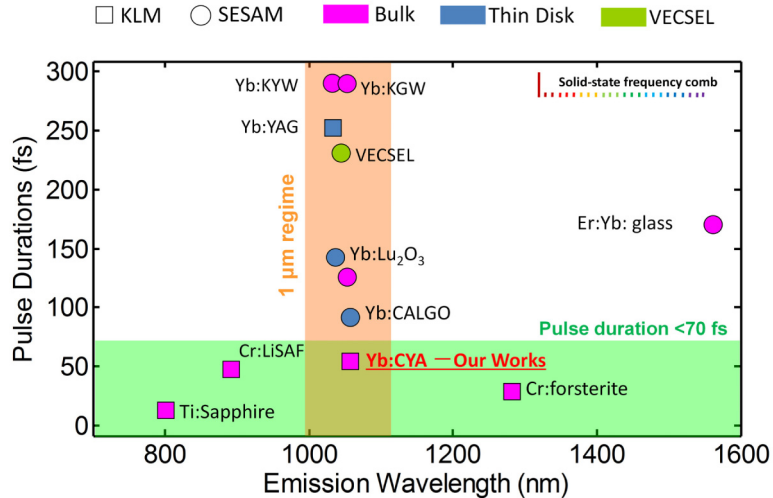


Fig. 1. Self-referenced solid-state frequency combs classified in terms of emission wavelength and pulse duration of the fundamental laser sources. Frequency comb from bulk Yb:CYA oscillator has the broadest output spectrum in the 1- μ m regime.

In this letter, we present the CEO stabilized Yb:CYA bulk OFC in the 1- μ m region. The fundamental oscillator we used is a fiber-laser pumped KLM Yb:CYA laser with output power of 250 mW and a pulse duration of 57 fs, which we believe to be the shortest pulse duration among 1- μ m solid-state OFCs. One octave-spanning supercontinuum was achieved by injecting only 58 mW mode-locked power into a 1.3-m-length photonic crystal fiber (PCF). The ultimate locked carrier-envelope offset frequency (f_{ceo}) has an integrated phase noise (IPN) of 316 mrad (from 1 Hz to 10 MHz) and Allan deviation of 5.6×10^{-18} (1-s gate time) for more than 4-hour recording. The good performances of our novel frequency comb can be attributed to the low phase noise and high stability of the Yb:CYA oscillator and our improvement to the conventional two-arm f - $2f$ interferometer, as will be described in the following section.

2. Experimental details

2.1 KLM Yb:CYA oscillator

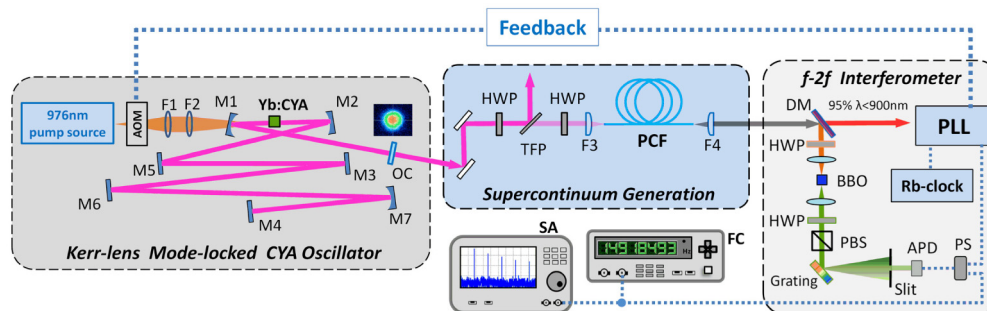


Fig. 2. Schematic diagram of the OFC from a KLM Yb:CYA laser. F1, F2: spherical lenses; F3, F4: aspherical lenses; M1-M7: high reflective mirrors; M3 and M4: Gires-Tournois interferometers (GTIs) with dispersion of -1000 fs^2 and -250 fs^2 ; AOM: acoustic optical modulator; OC: output coupler; HWP: half-wavelength plate; TFP: thin film polarizer; PCF: photonic crystal fiber; DM: dichroic mirror; PBS: polarization beam splitter; APD: avalanche photo diode; PS: power splitter; PLL: phase locked loop; SA: spectrum analyzer; FC: frequency counter. Rb-clock: Rubidium clock.

The OFC laser source we used is a KLM Yb:CYA oscillator as schematically shown in Fig. 2. The 3-mm-thick gain medium is mounted in a water-cooled copper heat sink which is maintained at 14 °C. Under pump power of 5.7 W, the typical output power is 250 mW with a central wavelength of 1048 nm, pulse duration of 57 fs and repetition rate of 83 MHz. The long-term power stability is less than $\pm 0.5\%$ for a 3-hour measurement. The mode-locked laser is vertically polarized with a polarization extinction ratio of more than 100:1. More specific parameters and mode-locked performances of the laser are described in detail in [31].

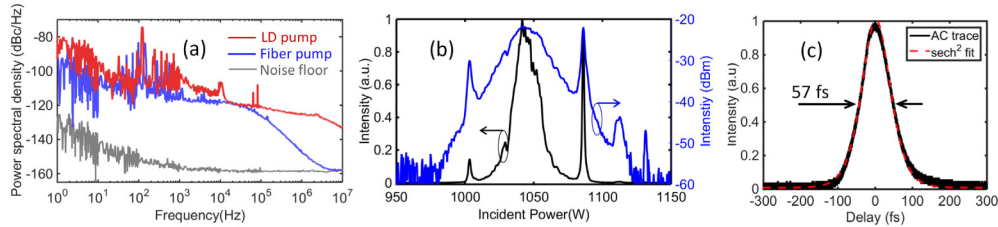


Fig. 3. (a) Relative intensity noise of the novel fiber source and traditional LD source; (b) mode-locked output spectra in linear scale (black line) and logarithmic scale (blue line); (c) the measured autocorrelation and fits for sech²-pulse.

In order to obtain a low noise source for the OFC, several factors are considered and improved for the Yb:CYA laser design. Theoretical and experimental researches have indicated that relative intensity noise (RIN) accompanying the pump source has considerable effects on operating properties and CEO linewidth of the mode-locked laser [32,33]. Particularly, for noise region of more than 1 kHz, pump fluctuation even could be the dominated noise source of an optical frequency comb system [34]. This high-frequency noise, however, cannot be well suppressed due to the limited feedback bandwidth of the common pump modulation method for CEO stability [35]. This leads our insight into the novel single-mode fiber source with intrinsic lower noise property, as shown in Fig. 3(a). Compared with the most widely-used laser diode (LD) pump, the fiber source has a better noise performance, especially in the tough high-frequency area. Meanwhile, the high brightness of the fiber pump decreases the heating effect in the pump absorption process, thus effectively restrains the noise introduced by the thermal expansion of the gain medium [36].

Another denoise measure we took is to reduce the intracavity residual loss, thereby decreasing the intrinsic quantum noise limit of the mode-locked oscillator [37]. In our experiment, we applied an output coupler with a transmission rate as low as 1.6% to increase the Q-factor of the laser cavity. Actually, pure KLM configuration can also avoid the additional losses introduced by mode-locking assisted elements, like saturable absorption mirror (SESAM) and topological insulator.

2.2 Supercontinuum generation

Part of the output pulses without further compensation or amplification are then launched into a commercial PCF (NKT, SC-3.7-975) for supercontinuum (SC) generation, as shown in Fig. 2. As the coupled power increased, the spectra were symmetrically extending around the incident central wavelength of 1048nm, and one-octave spectrum with a 700nm span would be finally achieved. With the assistance of the aspheric lens and high-resolution 3-axis adjusting stage, the fiber coupling efficiency could achieve up to 57% and the fluctuation within 3 hours is less than $\pm 1.3\%$.

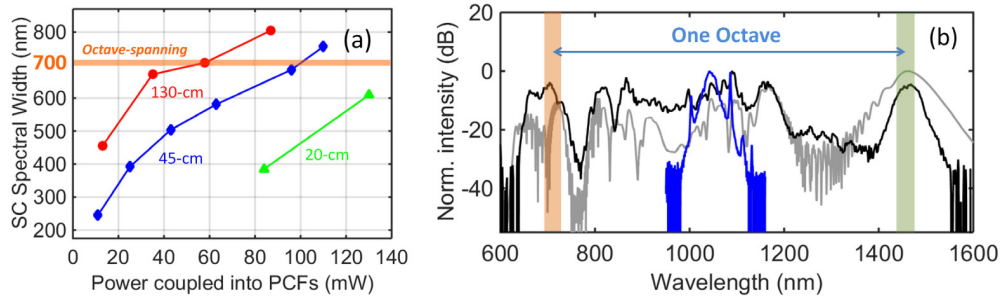


Fig. 4. (a) The spectral width versus power coupled into the PCFs, note: the PCFs with different lengths are the same type with 976 nm zero dispersion wavelength (ZWD); (b) The measured (black line) and simulated (gray line) SC spectra generated by a 1.3-m PCF, the blue line is the mode-locked output spectrum of the laser.

Three PCFs with different lengths were compared for the spectral broadening. The relationship between coupled pulse power and SC spectral width is revealed in Fig. 4(a). The one-octave threshold is measured to be only 58 mW for 1.3-m PCF. And the shortest PCF length for octave-spanning generation in our case is evaluated to be about 30 cm. Figure 4(b) describes the measured and simulated SC spectra generated by a 1.3-m PCF with coupled power of 58 mW. Two obvious peaks at the wavelengths of 700 nm and 1400 nm could be observed on the sides of the SC, which will be beneficial to the subsequent beating process for the f_{ceo} detection.

2.3 CEO detection and stabilization

Up to now, the most common setup for the CEO detection of the solid-state OFC is the two-arm f - $2f$ interferometer [4]. In this method, longer wavelengths are firstly divided from the SC for the second harmonic generation (SHG) and then recombined to beat with the shorter wavelengths. In our experiment, a simplified single-path f - $2f$ scheme [38] is employed as shown in Fig. 2. Octave-spanning SC generated by 1.3-m PCF shown in Fig. 4(b) is chosen for the CEO detection. Considering the SC intensity around 700 nm is higher than that around 1400 nm, 95% of the red light are firstly filtered out by a dichroic mirror (DM) to balance the intensity before they are reflected to the interferometer. Then the remaining SC is focused into a 3-mm BBO crystal for the frequency doubling of the infrared peak at 1400 nm. After that, the polarization of the doubled and fundamental 700 nm light is rotated and selected by a half-wavelength plate (HWP) and a polarization beam splitter (PBS) for the f_{ceo} beat signal detection.

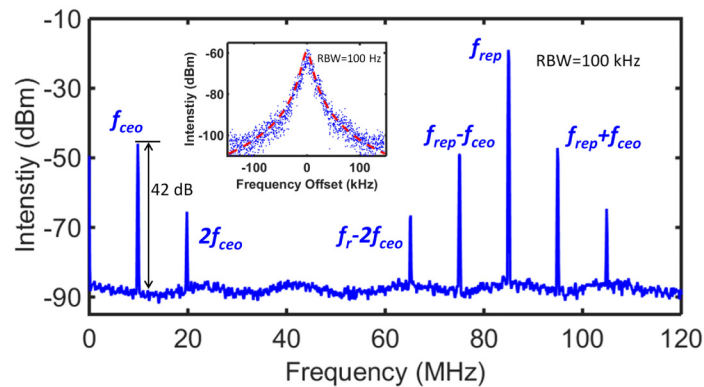


Fig. 5. Radio frequency spectrum with 42-dB SNR f_{ceo} beat signal (unaveraged, RBW = 100 kHz), f_{rep} : repetition rate; the inset: free-running f_{ceo} signal fitted with a 9.6-kHz FWHM square-Lorentzian line shape (RBW = 100 Hz).

One should note that, compared with the traditional f - $2f$ structure, there is no delay line in our configuration. The time delay between the infrared and red light, however, could be conveniently adjusted via changing the intracavity dispersion of the oscillator, like tilting the end mirror or the output coupler. This simplified collinear design, on the other hand, avoids the vibration noise introduced by the spatially overlap of the two arms, and accordingly, ensures the long-term stability during the CEO detection process.

Figure 5 shows radio-frequency (RF) spectrum measured by a frequency analyzer (R&S, FSW 26). The f_{ceo} signal has a signal-to-noise ratio of 42 dB under a resolution bandwidth (RBW) of 100 kHz, which is considerably higher than the typical value of 30 dB for common feedback electronics. Detailed distribution of the signal peak is revealed in 100-Hz RBW and fitted with a 9.6-kHz-FWHM square-Lorentzian line shape (inset of Fig. 5). Fitting curve of this kind was also adopted in a 1.5- μm solid-state OFC in [18]. Compared with the Lorentzian fit commonly used in the fiber OFCs, the square-Lorentzian fit features much narrower linewidth and lower wings beside the central peak, thus to be a more reasonable choice for the low-noise solid-state OFCs [17,18].

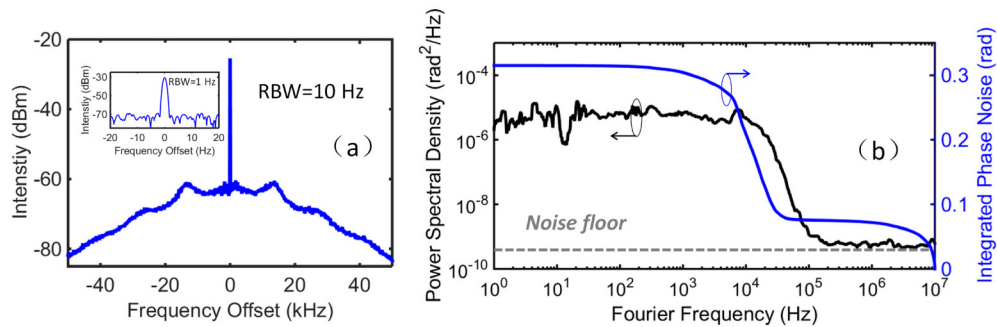


Fig. 6. (a) The frequency spectrum of the locked f_{ceo} signal; (b) phase noise and integrated phase noise of the locked f_{ceo} signal.

The beat signal obtained by the avalanche photodiode is feedback to the Yb:CYA oscillator for the CEO stability. An acoustic optical modulator (AOM) is employed as an actuator to fast adjust the pump power of the laser. The RF synthesizer, frequency analyzer and frequency counter are all referenced to an external Rb-atomic clock (Fig. 2). When the f_{ceo} is locked, a strong coherent spike will appear distinctly at the center of the beat signal, as shown in Fig. 6(a). The corresponding linewidth is narrowed from 9.6 kHz to be less than 1 Hz, which is the limit resolution of our frequency analyzer. More complete phase noise performance of the locked f_{ceo} signal is characterized by the power spectral density (PSD) in Fig. 6(b).

Although the phase locked loop (PLL) we used have a nominal 200 kHz bandwidth, the actual bandwidth of the whole feedback system is limited to be only 10 kHz by the upper level lifetime of gain medium (426 μs for Yb: CYA crystal) [35]. As a comparison, we also apply this servo electronics to stabilize a Ti:sapphire OFC with a similar configuration (3.2 μs for Ti:sapphire crystal), and the bandwidth in this case is found to be around 100 kHz [39]. Even so, the residual in-loop IPN of the controlled CEO (integrated from 1 Hz to 10 MHz) is calculated to be as low as 316 mrad (blue line in Fig. 6(b)), 70% of which originates from outside the servo bandwidth. The IPN value, therefore, is expected to be much smaller if fast modulation technique is adopted. And similar experimental verification has been demonstrated in [25] and [35].

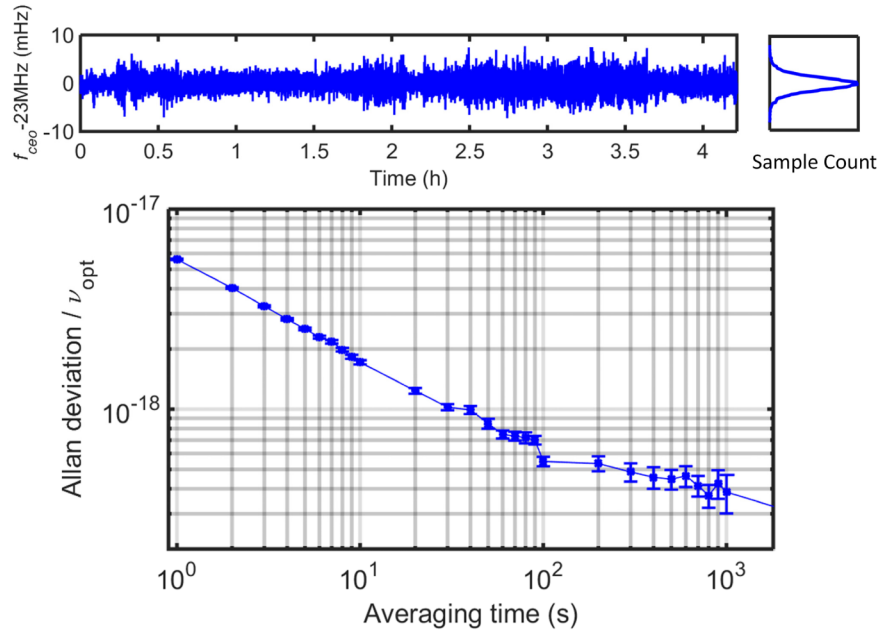


Fig. 7. The frequency deviation of the locked f_{ceo} signal for more than 4 hours recorded by the counter at 1-s gate time and the corresponding Allan deviation to the optical laser frequency ν_{opt} ($\lambda_{\text{opt}} = 1048\text{nm}$).

Furthermore, we investigated the long-term stability of the locked f_{ceo} . The frequency offset from a 23-MHz reference was recorded for more than 4 hours (the upper panel of Fig. 7) and the standard deviation is calculated to be 1.6 mHz. This value, to our knowledge, is the best one for the solid-state OFCs in the 1- μm region. The inset to the right is the frequency distribution histogram of the recorded sample with a 4-mHz FWHM, which indicates a narrow linewidth of the locked f_{ceo} signal. The Allan deviation corresponding to different averaging time is shown in the lower panel of Fig. 7. The value with 1-s gate time is only 5.6×10^{-18} at the central wavelength of 1048 nm, which is comparable to the state-of-the-art Ti:sapphire OFC. The long locking time and high stability of our comb show the robustness and reliability for the application in the future.

3. Conclusion and outlook

We report a CEO controlled OFC based on a KLM bulk Yb:CYA laser with the emission wavelength around 1 μm . Low-noise fiber pump source and high-Q cavity improved the noise performance of the oscillator. The use of the collinear f - $2f$ interferometer not only simplified the setup and adjustment, but also enhanced the stability in the CEO detection process. After several improvements mentioned above, CEO stabilized OFC with an IPN of 316 mrad (from 1 Hz to 10 MHz) and Allan deviation of 5.6×10^{-18} (1-s gate time, at 1048 nm) was obtained. The final long-term results with low timing jitter indicate our novel OFC to be a potential candidate for high precision measurement, low-phase-noise microwave generation and so on.

As mentioned above, gain-dependent f_{ceo} -stabilization method to a great extent is subject to gain media response speed to the pump intensity, particularly for doped ions with longer upper level lifetime such as Yb^{3+} and Er^{3+} . Therefore, in order to accomplish lower f_{ceo} noise performance, new denoise techniques have to be utilized to circumvent this feedback process. For high-gain lasers like fiber lasers and thin disk lasers, electro-optic and acoustic-optic modulators can be inserted into laser cavity to directly modulate the intracavity loss to obtain a broader bandwidth [25,40]. This method, however, is more challenging for a KLM bulk laser, where the introduction of extra dispersion and high losses will have a larger influence on the mode-locked state. The electro-optic modulated graphene and opto-optic modulated

SESAM were demonstrated to process very low nonlinearity, dispersion and insertion loss [35,41], but they are still not commercially available so far. In contrast, self-referenced feed-forward approach [42], which is characterized extracavity f_{ceo} modulation, is an ideal proposal to us. In this method, an acoustic optical frequency shifter (AOFS) is employed to directly suppress the f_{ceo} phase noise of the output laser, providing MHz feedback bandwidth without interrupting the free-running state of the oscillator. Its simple locking electronics would also reduce the complexity of the OFC. With this method, the residual phase noise of our locked f_{ceo} , we believe, could further decrease to the level of dozens of mrad.

Acknowledgments

This work is partially supported by the National Basic Research Program of China (973 Program Grant No.2012CB821304), and the National Natural Sciences Foundation of China (Grant No. 11078022, 61378040).